Axiomatic principle of multi field coupling dynamics analysis

Peng Yue[1,2]*, Jinghui Zhang[2], Sibei Wei[3], and Bin Chen[3,4]*

[1] *School of Physics and Optoelectronics, Ocean University of China, Qingdao, Shandong 266100, China*

[2]*School of Aeronautics and Astronautics, University of Electronic Science and Technology of China, Chengdu, Sichuan 611731, China*

[3] *Center for High Pressure Science & Technology Advanced Research (Shanghai), Shanghai 201203, China*

[4]*Harbin institute of technology, Shenzhen, Guangdong 518055, China*

**Corresponding author*

A multi-field coupling system involves several physical quantities and is usually difficult to achieve satisfactory performance in practice due to the lack of merit index for such complex system. Here, we propose a gauge, the field-exchange rate (FER), for evaluating and guiding the design of a multi-field coupling system. Basically, the FER of a physical quantity determines the allowed strength of that quantity loaded in the system. The best performance and reliability of the system can be achieved if the FERs of all relevant physical quantities are satisfied. The application of this FER gauge in previously reported studies generates the data that is consistent with the experimental results, which verify the validness of our FER approach. In addition, our FER analysis predicts that for electromagnetic launch techniques aluminum is a better candidate material than copper, a conventionally and widely chosen material in today's industry applications. Our ampere force experiment confirms this selection suggested by FER gauge. It can be expected that FER gauge would become a powerful and convenient tool in designing advanced and complicated systems with optimal performance in modern industries.

I. Introduction

In the first industrial revolution, the steam engine bridged heat and mechanics, and many new industries were thus established. Since then, significant progress has been made in the research of multi-field coupling. For instance, electromechanical, electrothermal, photoelectrical materials and other multi-fields coupling materials have been studied and developed for energy utilization, environmental protection, industrial production and other fields. The energy conversion between different physical fields is very usual in many industry problems. On the control of mechanical properties in laser additive manufacturing, Kürnsteiner [2] et al. believed rapid quenching, sequential in situ heating and local phase transformation can be used to produce layered microstructure to achieve precise and local control of the formation and precipitation of martensite, thus controlling the mechanical behavior. Regarding the improvement of the conversion efficiency of thermoelectric devices, Hinterleitner [3] et al. used magnetron sputtering to prepare the thin film Heusler alloy based on Fe2V0.8W0.2Al, which has high thermodynamic and electrical properties, has good thermoelectric properties, and can greatly improve the conversion efficiency of thermoelectric

devices. At the same time, in the utilization of solar energy, Min [4] et al. stabilized the black α phase of formamidine-based lead triiodide (FAPbI3) in perovskite solar cells by doping methylene diamine dichloride (MDACl2) to ensure that its inherent band gap does not expand and its thermal stability achieves a photoelectric conversion efficiency of up to 23.7%. Recently, elastic thermal refrigeration has become a frontrunner in non-vapor compression refrigeration technology. Hou [5] et al. had constructed highly efficient, thermodynamically efficient, ultra-narrow hysteresis elastomeric refrigeration materials by additive manufacturing of Ti-Ni alloys, which are 4 to 7 times more efficient than usual. Moreover, the reversible and repeatable elastic thermal cooling properties of the titanium-based alloy material keep stable in one million cycles. In terms of improving the strength of single-phase high-entropy and medium-entropy alloys, Yang [6] et al. regulated its transition the transition from fcc-austenite to body-centered cubic (bcc) martensite can be adjusted, constraining it to remain as metastable fcc after quenching through the transformation temperature. During the stretching process, the matrix gradually transforms into bcc-martensite to achieve a significant increase in material strength. However, the conservation relationships that should be followed in multiple fields have not yet been clarified, resulting in a lack of in-depth understanding of the essence of nature.

Although multi-physics field coupling is broad and significant, the current research is usually done by trial-and-error methods [7,8], and so, the cost of exploration is usually high and the solution is often not optimal or satisfactory. For more efficient and effective explorations, a general rule governing multi-field coupling is needed. In this article, we present our theory on multi-physics field coupling, followed by the experimental confirmations and prediction verification.

II. The field-exchange rate (FER) of a multi-field coupling system

From the perspective of the development of physics in the past hundred years, physics has repeatedly proven a viewpoint that the change in the microstructure of matter is one of the direct factors influencing the alterations in the material state and physical processes of an object. Understanding the material state and physical processes when multiple physics fields interact is crucial in physics. These changes often entail intricate combinations of different physical fields, making it essential to unravel their complexities. This exploration is instrumental in deciphering the underlying causes of significant physics problems. We can analyze the correlation of the influence of the microstructure of matter on physical quantities, which are quantities in physics that measure the properties of matter or describe the state of motion of objects and their change processes.

In an isolated system with an unchanging external environment, when the microscopic structure of matter changes, the first affected physical quantity Φ can be called the matter quantity Υ, such as material density ρ_m, charge density ρ_q, current density ρ_I, momentum ρv_i, or

kinetic energy E_k, etc. Subsequently, the physical quantity Φ of the change of the surrounding environment caused by the change of matter quantity Υ can be called the environmental quantity μ, such as geometric parameters r, electric field intensity E, magnetic field intensity H, etc. Lastly, the physical quantity Φ that is formed by the interactions between environmental quantity μ and other matter quantity Υ can be called the action quantity Π, such as force F, torque M, or potential energy E_p etc.

The action quantity Π represents the impact of the original object on the objects within the surrounding environment of the original object. In general, the state of matter or physical processes are mainly affected by matter quantity Υ and action quantity Π. Additionally, it is essential to follow the conservation of physical quantities, such as mass, charge, momentum, angular momentum, and energy etc., in order to establish a material state or initiate a physical process. Hence, through abstract mathematical models, we can make astonishing interpretations and unifications of the universal conservation laws, thereby discovering new laws and methods [9].

1. Definition of density and flux density of physical quantity

Within this framework, the magnitude of a physical quantity per unit of measurement can be defined as the density of the physical quantity ρ^{Φ}. Depending on the object and form of the quantity, the measure τ in the definition of the density of the physical quantity ρ^{Φ} can be area, volume, length or other measurement, which should be selected according to the specific object of action and the analysis process. In simple terms, the density of physical quantities can be used to visually describe the spatial distribution of a certain physical quantity Φ

$$\rho^{\Phi} = \frac{\delta\Phi}{\delta\tau}, \tag{1}$$

here, $\delta\tau$ is the changes in spatial measurement (such as volume, area, and length, etc.). The matter quantity Υ can be expressed by the density of matter quantity ρ^{Υ}

$$\delta\Upsilon = \rho^{\Upsilon}\delta\tau. \tag{2}$$

Simultaneously, considering that the action quantity Π is typically the result of the interaction between the environmental quantity μ and the matter quantity Υ, it can generally be expressed in the form of physical quantity density

$$\rho^{\Pi} = \mu\rho^{\Upsilon}. \tag{3}$$

It is worth mentioning that the correlation between the matter quantity Υ and environmental quantity μ may not always be present. To illustrate, there have been no findings indicating any interaction when the current intensity is exposed to a gravitational field. In general, whether the density of matter quantity ρ^{Υ} and environmental quantity μ can interact to form the density of action quantity ρ^{Π} is determined by the experimental results, for example, since

$$G = gm \Rightarrow \frac{\mathrm{d}G}{\mathrm{d}\tau} = g\frac{\mathrm{d}m}{\mathrm{d}\tau}$$

so accordingly, in a more generally way, we can introduce the density of any matter-based quantity and any interaction-based quantity. Furthermore, in line with equation (1), the change of action quantity $\delta\Pi$ can also be expressed as

$$\delta\Pi = \mu\rho^{\Upsilon}\delta\tau\,. \tag{4}$$

In general, if we designate the environmental quantity μ as 1, the action quantity Π will match the matter quantity Υ in numerical terms, as the shown in equation (2).

As the matter quantity Υ and action quantity Π are physical quantities directly influencing the matter state or physical processes, we can derive a more generalized description method. In other words, when it comes to the physical quantity P that have a direct impact on the matter state or physical processes, we can describe its change as

$$\delta P = \mu\rho\delta\tau\,, \tag{5}$$

here, μ is the environmental quantity, ρ is the investigation object's density of matter quantity, and $\rho = \rho^{\Upsilon}$. When $\mu = 1$, this physical quantity is the matter quantity $P = \Upsilon$, that is, the physical quantity directly affected by microscopic structural changes; When $\mu \neq 1$, the physical quantity is the action quantity $P = \Pi$, that is, the physical quantity of the interaction between the matter quantity Υ and environmental quantity μ.

In order to study the physical process under temporal change, it is common to treat the temporal rate of change of a physical quantity as a new physical quantity. The temporal rate of change of a physical quantity with the density of space can be called the flux density of physical quantity ρ_f^{Φ}. And according to equation (1), there is

$$\rho_f^{\Phi} = \frac{\delta}{\delta\tau}\left(\frac{\mathrm{d}\Phi}{\mathrm{d}t}\right). \tag{6}$$

Similar to the analysis method of physical quantity density, according to equation (5), we can obtain a more general description for flux density, that is, for a physical quantity P that directly affects the matter state or physical process, the change rate over time can be described as

$$\delta\frac{\mathrm{d}P}{\mathrm{d}t} = \mu\rho_f\delta\tau \tag{7}$$

here, μ is the environmental quantity and ρ_f is the investigation object's matter flux density, $\rho_f = \rho_f^{\Upsilon}$. When $\mu = 1$, this physical quantity is the matter quantity $P = \Upsilon$, that is, the physical quantity directly affected by microscopic structural changes; When $\mu \neq 1$, the physical quantity is the action quantity $P = \Pi$, that is, the physical quantity of the interaction between the matter quantity Υ and environmental quantity μ. As time and space are managed in a similar manner, there is no discernible disparity when it comes to the sequence of mathematical operations, therefore,

$$\frac{\mathrm{d}\delta P}{\mathrm{d}t}=\delta\frac{\mathrm{d}P}{\mathrm{d}t}. \tag{8}$$

From equation (5) we can obtain

$$\frac{\mathrm{d}\delta P}{\mathrm{d}t}=\mu\left(\frac{\mathrm{d}\rho}{\mathrm{d}t}+\frac{\rho}{\mu}\frac{\mathrm{d}\mu}{\mathrm{d}t}+\rho\theta\right)\delta\tau. \tag{9}$$

Let $\vec{v}$ represent the rate of change in measurement τ over time, then $\theta=\nabla\cdot\vec{v}$ signifies the divergence in the change of measurement τ, illustrating the degree of spatial expansion and contraction over unit time. By comparison with equation (9), we can determine the relationship between flux density and density of a physical quantity

$$\rho_f=\frac{\mathrm{d}\rho}{\mathrm{d}t}+\frac{\rho}{\mu}\frac{\mathrm{d}\mu}{\mathrm{d}t}+\rho\theta \tag{10}$$

Moreover, the above analysis mainly considers the magnitude of the physical quantity. To fully account for the orientation of the physical quantity, it is essential to incorporate the covariant density ρ_e of that attribute in the direction perpendicular to the Cartesian coordinate system.

$$\rho_e=\rho\frac{|\vec{v}|}{r}. \tag{11}$$

Through the analysis of equations (5), (7), and (9), it becomes apparent that the density and flux density of matter are intricately linked not only to the nature of the matter itself, but also to the geometric shape of its distribution in the measurement space. Thus, by tracking the changes in the microscopic structure of matter and its reciprocal effects on the surrounding matter, and using the interdependencies between the matter quantities, the environmental quantities, and the action quantities, we can more easily articulate the essential rules of a matter state or a physical process. By providing a description that seamlessly connects the macroscopic and microscopic aspects of the physical world, it becomes more feasible to uncover the underlying principles that govern material phenomena and microscopic structures. For example, the scenario where the minuscule composition of an object undergoes a transformation; as a result, its temperature field is altered, consequently impacting the heat field in its vicinity. The temperature of the environment plays a crucial role in shaping the behavior of other substances present, with conduction, convection, and radiation being among the ways through which this influence is manifested. As a consequence, the object undergoes modifications at the microscopic level. Additionally, looking at it from an engineering standpoint, creating a direct link between the larger and smaller scales would greatly streamline the process of selecting materials for mechanical design.

2. Definition of field-exchange rate (FER)

The major obstacles encountered when researching in multi-physics fields stem primarily from the considerable discrepancies in how each physics field is portrayed. In many ways, the notions of physical quantity density and flux density have effectively dealt with the task of describing multi-

physics fields in single-body systems. Nonetheless, substantial discrepancies can be observed in the transfer of energy within intricate systems involving multiple bodies, owing to the fact that each individual body undergoes distinct mechanical forces and movements. To establish connections between different aspects of physics and specific elements within an intricate system, it is crucial to develop a novel dimensionless physical parameter and employ the principles of conservation laws or equilibrium equations.

The field-exchange rate (FER) can be mathematically expressed as:

$$z = \frac{\mu}{g}\frac{\rho_i}{\rho_m}, \tag{12}$$

where ρ_i signifies the density or flux density of the conservation physical quantity of the i-th field, μ signifies the excitation field in which the substance resides, ρ_m signifies the material density of the affected substance, and g represents the gravitational acceleration. And the FER is the ratio of a certain physical quantity to the force or torque exerted by gravity over a distance of 1 meter, in a time of 1 second, or equivalent to the torque exerted for 1 second within a 1-meter range.

3. Law of conservation of FER

The different interpretations mainly stem from the choice of conservation laws. It is worth noting that this definition makes FER a dimensionless parameter that can represent the degree of interaction of a physical quantity. In this way, we can derive a more universal conservation law in physics, namely the conservation of FER in multi-physics field .

When a substance is subjected to the coupled action of multi-field, the FER transfers from one physical field to another or from one part of the substance to another. The total FER remains constant throughout the spacetime evolution, i.e.,

$$z_{\sum}\left(x_i, t\right) = \text{const} \tag{13}$$

here, x_i represents spatial parameter, t represents temporal parameter.

To better understand FER, we can analyze several cases involving the coupling of different fields. Typically, environmental exposure and in-service wear impact the mechanical performance of engineering materials, and the mechanical performance of materials may vary due to the environment in which they are used. Mathematically speaking, the physical meaning of everything that can be described as an equation is to describe the equilibrium process of a system. Therefore, identity equation necessarily means a conservation characteristic of nature. With this understanding for the sample space, we can get conservation of uncertainty in nature. To help gain a better understanding, let's use hot pressing as a schematic diagram to demonstrate how FER works. (Figure 1).

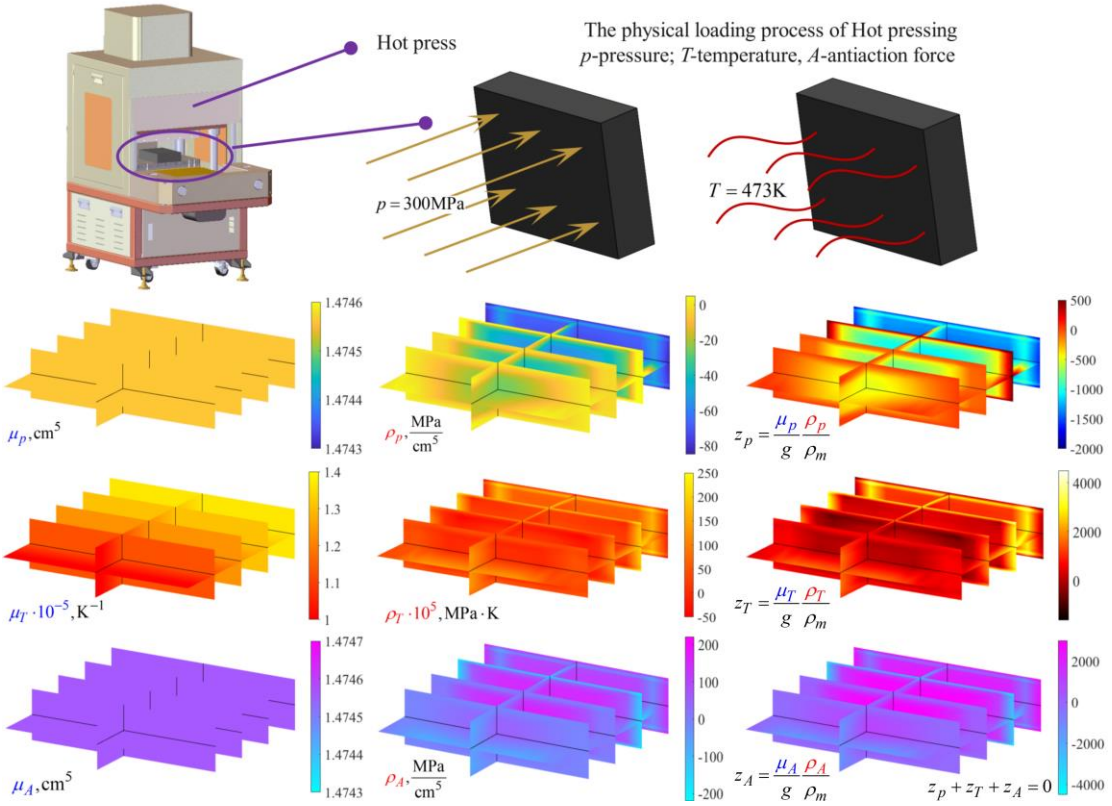

Figure 1. The schematic diagram of the principal stress field's physical quantity density and FER in the hot pressing process. μ_p 、 μ_T and μ_A represent the environmental quantities distribution of the pressure field, thermal field, and reaction force field respectively; ρ_p 、 ρ_T and ρ_A represent the distribution of the principal stress field's matter density caused by the pressure field, thermal field, and reaction force field, respectively.; z_p 、 z_T and z_A represent the FER distribution of the pressure field, thermal field, and reaction force field respectively. When the material undergoes hot pressing, we can clearly observe that the sum of the FER in the pressure, thermal, and reaction force fields is always zero at any point.

III. Applications of the FER in multi-field coupling systems

Before dealing with individual applications, we expand the basic concepts of FER theory to the several fundamental forces. In the well-established domain of physics, typical physical quantities, such as universal gravity, coulomb force, ampere force, thermal stress and so on, can be described using FER expressions (Table 1).

Table 1. The FER expressions of common physical quantities, blue represents the environmental quantity, while red represents the physical quantity density.

Physical quantities	FER expressions	Description of physical quantities
Universal gravity	$z = \frac{P}{g}\frac{\rho_m}{\rho_m}$, $P = \frac{GM}{r^2}$	g is the gravitational acceleration; ρ_m is the density of star; G is the universal gravitational constant; M is the mass of star; r is the

		distance between two stars.
Coulomb force	$z=\frac{K}{g}\frac{\rho_q}{\rho_m}$, $K=\frac{kQ}{r^2}$	g is the gravitational acceleration; ρ_q is the density of charge; ρ_m is the density of star, k is the Coulomb's constant; Q is the amount of charge, r is the distance between two charges.
Lorentz force	$z=\frac{L}{g}\frac{\rho_q}{\rho_m}$, $L=vB$	g is the gravitational acceleration; ρ_q is the density of charge; ρ_m is the density of star, k is the Coulomb's constant; v is the velocity of charge, B is the magnetic flux density.
thermal stress	$z_f=\frac{\kappa}{g}\frac{\rho_T}{\rho_m}$, $\rho_T=\Delta T$	κ is the coefficient of thermal conductivity; g is the gravitational acceleration; ρ_T is the temperature distribution density; ρ_m is the density of star, ΔT is the amount of temperature change per unit measurement.

Note: Since the essence of physical quantity density is the fundamental property of matter, if a physical quantity is a concentrated quantity, it should be classified as an environmental quantity. But this is not absolute. If it is found that the variation of a physical quantity in material space is intolerable, then the physical quantity should be written as one of the material properties in the physical density.

FER analysis is feasible for all applications related to various fields, and this method can be followed to establish relevant basic models in various fields. Here we describe these problems through two examples.

Application 1: Example of electromechanical coupling

The coupling between force and electric fields has promoted the rapid development of electromechanical materials, such as new C/C composites [10] and Gd_2O_3-doped CeO_2 (CGO)-based electrostriction materials [11]. These progresses reconcile the ultrahigh strength and high conductivity of materials [10,11], and improving the flow stress and ductility of structural materials [12]. Jin *et al.* [12] maximized the influence of surface processing by utilizing nanomaterials with an extremely large surface area. Secondly, they designed the material as a hybrid material, in which the electrolyte becomes an intrinsic part of the microstructure. In the experimental process, they first obtained samples with uniform nanoscale porous structure through dealloying, then used 1M $HClO_4$ solution with weak adsorption capability on gold to infiltrate the pores, and finally conducted compression tests under the control of an in-situ electrochemical device. Their conclusion indicates that the interface properties and processes can be controlled by electrical potential, thereby influencing the macroscopic behavior of nanocomposite materials. Through this approach, the yield

strength and flow stress of their materials can exhibit recoverable changes of up to 2 times.

This is a classic example of a multi-field coupling problem, involving the coupling of electric field, force field, chemical field, and thermal field. These fields exhibit obvious characteristics of energy flow, where electric potential energy is converted into chemical energy and thermal energy, while also providing strain energy and surface energy for the sample. To simplify the mathematical description of the processing and make the physical processes more understandable, we adopt commonly used engineering methods by introducing the efficiency η of electrical energy and chemical energy to eliminate the dissipation of thermal energy and other energies. Although this may result in some loss of accuracy, it makes the main contradictions clearer and simplifies the problems behind. In this case, there is a clear time effect, so we describe the conservation of FER in the system using flux density, and we can derive:

$$\rho_f^{\varepsilon} + \rho_f^{s} = \eta\left(U\rho_f^{e} + \varsigma\rho_f^{c}\right), \tag{14}$$

where ρ_f^{ε} represents the strain energy flux density of the material, ρ_f^{s} represents the surface energy flux density of the material, ρ_f^{e} represents the electrical energy flux density, U represents the scanning voltage in cyclic voltammetry, ς represents the chemical potential of the electrolyte solution, and ρ_f^{c} represents the chemical energy flux density.

In general, solutions with concentrations below 1M can be classified as dilute solutions, while solutions with concentrations above 6M can be classified as concentrated solutions. In this case, a 1M $HClO_4$ electrolyte solution is used, and considering that dilute perchloric acid generally does not react with metals while concentrated hot perchloric acid can react and even dissolve gold electrodes, we can infer that the electrolyte solution used in the experimental process satisfies the theory of dilute solutions. The equation for the electrode reaction is $Ag_{(s)} + Cl^- - e^- = AgCl_{(s)}$, Since the temperature change caused by the reaction heat is small, we neglect the effect of temperature change and assume that temperature and diffusion coefficient remain constant. Additionally, we assume that the chemical reaction rate does not change and that the reaction is in chemical equilibrium, thus the rate of change of chemical potential with respect to time is zero.

Considering that the temperature variation of the sample mainly arises from the temperature changes in the chemical reaction and the temperature changes caused by electrical energy, these temperature changes are generally considered to be slow. The temperature variation directly affects the intermolecular forces, which in turn affect the surface tension. Therefore, we assume that the flow of surface energy is uniform, resulting in a linear relationship between the variation of surface tension and time. Taking into account the uniform variation of potential with time in cyclic voltammetry, the basic differential expression for this work is established as:

$$E\varepsilon\vartheta\frac{\mathrm{d}\varepsilon}{\mathrm{d}U}-\zeta\vartheta^2\left(\frac{\mathrm{d}\varepsilon}{\mathrm{d}U}\right)^2=\frac{\eta}{L}\left(U\rho^I+\int_U\rho^I\mathrm{d}U\right)+\eta\varsigma\rho_f^c-\rho_f^s\,, \tag{15}$$

where E is the Young's modulus of the material, ζ is the viscosity coefficient of the material, ε is its strain, ϑ is the scan rate of cyclic voltammetry, ρ^I is the current density of the electrolyte solution, and L is the effective length of the material perpendicular to the current flow surface. Using the finite difference method, we can obtain the theoretically predicted conclusions (Figure 2).

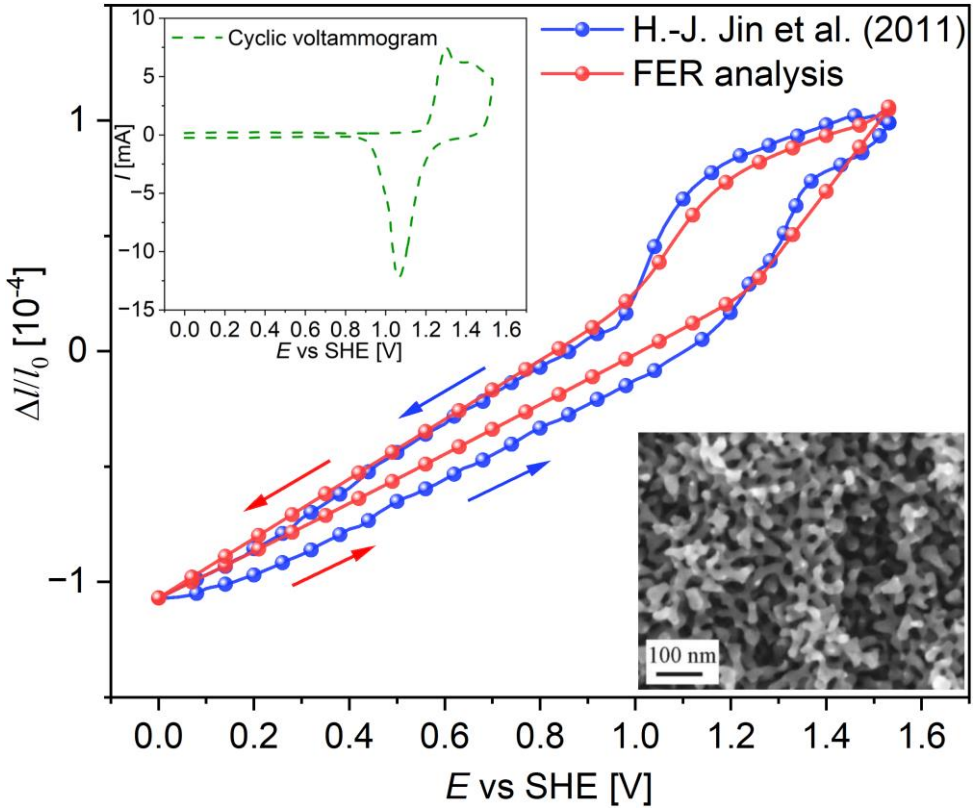

Figure 2. Response to a potential scan at 10mV/s in 1M $HClO_4$ solution, where the blue line represents the conclusions from the experiment conducted by Jin *et al*. [12], the red line represents the model studied by FER conservation, and the green dashed line represents the cyclic voltammogram measured during the same scan period. The average difference of approximately 10% between the experimental results and ours may come from the assumptions we used for simplification.

When the right side of the FER conservation equation (14) is a determined relationship, the left side represents the sum of surface energy flux density and strain energy flux density. When the surface effect decreases, further enhancement of the volumetric effect is needed, which requires increasing the elastic expansion of porous solid materials, in accordance with the conclusion obtained by Jin *et al*. [12] in their final experiment. Although we do not have the complete experimental details and input experimental data of this study, the results we obtained from our FER theory are in good agreement with the experiment.

Application 2: Example of thermoelectric coupling

In todays, approximately 90% of the world's electricity is generated by fossil power plants. Sustainable electrical power is one of the significant challenges of this century, and some solutions, such as thermoelectric cooling technology [13] and heat pumps [14], have been explored. It has been confirmed by many studies that thermoelectric modules can convert a portion of low-grade waste heat into electricity, thus enhancing the utilization efficiency of fossil energy [15,16,17,18]. The coupling between the thermal field and the electrical field directly affects energy utilization. Their efficiency depends on the thermoelectric figure of merit of their material components, which is a function of the Seebeck coefficient, electrical resistivity, thermal conductivity, and absolute temperature. Increasing the thermoelectric figure of merit has been a challenge over the past fifty years [15,16,17,18]. Due to the interdependence of the relevant parameters of the thermoelectric figure of merit, it is difficult to assess them directly. However, recent studies have indicated that nanomaterials can effectively enhance the thermoelectric figure of merit.

Hochbaum *et al.* [15] found that the Seebeck coefficient and electrical resistivity values of large-area, wafer-scale rough silicon nanowires with diameters ranging from 20-300 nm are similar to those of doped bulk silicon. However, for nanowires with a diameter of around 50 nm, the thermal conductivity is reduced by a factor of 100, resulting in a *ZT* value of 0.6 at room temperature. For such nanowires, the contribution of the lattice to thermal conductivity approaches the amorphous limit of silicon, which cannot be explained by current theories. Hence, Hochbaum *et al*. [15] carried out numerous experiments and calculations. They initially synthesized wafer-scale arrays of rough silicon nanowires using an electroless etching (EE) method at room temperature (295K). Next, the samples were rinsed with concentrated nitric acid for at least one hour to remove any residual Ag on the surface of the nanowires. Finally, the silicon nanowires were fixed on a suspended SiN_x membrane in parallel, and their thermal conductivity and other characteristics were measured using a measurement device. The results showed that, at room temperature, silicon nanowires with a diameter of 50 nm processed using wafer-scale fabrication techniques can achieve a thermoelectric figure of merit of 0.6. By optimizing doping, reducing diameter, and controlling roughness, the thermoelectric figure of merit could potentially be further increased. This enhancement in the thermoelectric figure of merit can be attributed to the effective scattering of phonons throughout the entire phonon spectrum by introducing nanoscale structures of varying length scales (diameter, roughness, and point defects).

FER analysis can be used to deal with the coupling between electric field and thermal field. In this work, the thermal conductivity coefficient, voltage, resistivity, and heat flux are all independent of time. So, if the temperature is constant, their physical states do not change over time and time

effects can be neglected. Taking into account the evident energy flow characteristics of the two fields, the conservation relation of the FER in the system can be described using physical quantity densities, resulting in:

$$k\rho^T = \frac{U^2}{l^2}\left(\rho^R\right)^{-1}, \tag{16}$$

where k is the thermal conductivity coefficient, ρ^T is the heat transfer energy density, U is the potential difference, l is the length of the silicon nanowire, and ρ^R is the resistivity.

In addition, through simple mathematical deduction, the Seebeck coefficient can be expressed simply as:

$$S = \frac{1}{2} l\varepsilon\alpha \,. \tag{17}$$

It can be observed that the Seebeck coefficient is closely related to the temperature derivatives of thermal conductivity coefficient, heat transfer density, and resistivity. Therefore, we define a new coefficient to characterize a certain feature of the physical quantity. In this case, the thermoelectric figure of merit can be expressed as:

$$ZT = \frac{S^2 T}{k\rho_R} = \frac{1}{4} l^2 \alpha^2 \rho^T T \,. \tag{18}$$

In this equation, $\varepsilon = \sqrt{k\rho^T \rho^R}$ represents the equivalent field strength, while α denotes the temperature coefficient, which is composed of three components:

$$\alpha = \frac{1}{k}\frac{\mathrm{d}k}{\mathrm{d}T} + \frac{1}{\rho^R}\frac{\mathrm{d}\rho^R}{\mathrm{d}T} + \frac{1}{\rho^T}\frac{\delta\rho^T}{\delta T} \,. \tag{19}$$

In physics, the temperature coefficient treated as the sum of the rates of change of the thermal conductivity coefficient, resistivity, and heat transfer energy density with respect to temperature. Experimental evidence has confirmed [19] that the angular frequency in phonon transport processes is related to the temperature gradient, and the heat transfer energy density is an important physical quantity that characterizes phonon transport and scattering. Upon directly extracting the relevant data and substituting it into equation (18) for calculation, we obtained the results with an average difference of below 5% with regard to the experimental results (Figure 3). We note that the magnitude of temperature gradient is influenced by factors such as heat transfer mode, heat transfer medium, heat transfer area, and heat transfer distance. Therefore, the heat transfer energy density typically varies due to the influence of material parameters such as lattice defects, diameter, and roughness. This leads to a significant reduction in thermal conductivity of Si nanowires, which is consistent with the conclusions drawn by Hochbaum *et al.* [15]. In other words, besides the consistency in terms of numerical values, the FER analysis can reveal the physics deep behind.

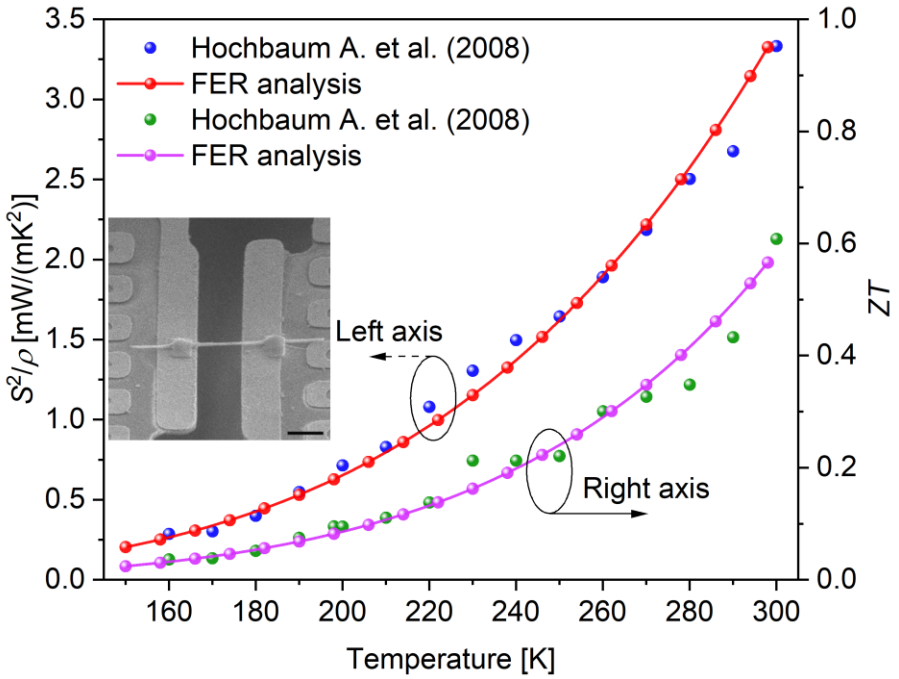

Figure 3. The thermal and electrical properties as well as the thermoelectric figure of merit calculations for silicon nanowires approaching 50 nm. The blue and green circles represent the experimental and calculated results from Hochbaum *et al*. [15], while the red and purple circles with lines represent the predicted data obtained through FER analysis.

IV. Confirmed FER prediction for the choice of candidate material of electromagnetic launching

In theory, the essence of engineering component design lies in ensuring that the maximum load-bearing capacity of the structure is greater than or equal to the maximum value of the functional load, which signifies the success of the component design. There is a significant contradiction here, as excessively large structures can result in increased costs, energy wastage, or significant impairment of functionality. Therefore, evaluating the quality of component design from the perspective of multi-field coupling primarily depends on whether the structure, functionality, information, and energy are appropriately matched. Due to the significant gap between physical quantities at present, making it unfeasible to achieve this, mechanism design typically follows a sequential iterative design process. This approach significantly prolongs the design cycle and reduces design efficiency.

The essence of mechanical design is the process of designing suitable structures to achieve mechanical functions. So, generally speaking, mechanical design is the process of gradually meeting the requirements of mechanical functional design and mechanical structural design. Assuming that the materials have been determined, the mechanical functional design or mechanical structural design can be analogized as a permutation and combination problem. Simply put, if all geometric

forms that meet the conditions are regarded as small balls, then both mechanical functional design and mechanical structural design are the process of selecting one from a pile of small balls. Therefore, the mechanical structure design process and the functional design process can be described by the probability distribution in a sample space.

FER is similar to the probability density value of this probability distribution. The process of mechanical design can be seen as the maximum FER value obtained from the intersection area between the probability density distribution of mechanical function design and the probability density distribution of mechanical structure design. At this point, we must establish the concepts for the FERs of the functional z_f and structural z_s physical field.

As shown in Figure 1, FER is a function of spatial distribution density or flux density, which effectively integrates the effects of different physical fields, ultimately achieving the integration of functionality and structure. Therefore, FER plays a crucial role in the field of applied physics by facilitating the desired parallel design method sought by industrial designers. It enables simultaneous exploration of different fields and, ultimately, through FER conservation, leads to finding the optimal design solution. Performing dynamic analysis of multi-physics coupling cases using FER allows for the examination of functional and structural fields in terms of dynamics, resulting in the derivation of fundamental dynamic equations based on FER. Taking electromagnetic propulsion as a current popular example, utilizing FER conservation allows for the derivation of the FER conservation equation for this force-electricity multi-physics coupling mechanism:

$$\frac{z_f}{z_s} = \frac{1}{1-\theta}, \theta = \frac{m}{M}, \tag{20}$$

where z_f represents the FER of the functional field, z_s represents the FER of the structural field, and θ denotes the mass proportion. The FER curves of different candidate materials under specific magnetic field conditions can be obtained based on the equation (20). Considering that copper and aluminum are the main materials used in the empirical selection of electrical materials, the FER curves for copper and aluminum are depicted in Figure 4a. Furthermore, based on FER conservation, the FER curves of the functional and structural aspects of the multi-field coupling mechanism can be obtained, as shown in Figure 4b.

Based on Figure 4b, it can be observed that copper cannot simultaneously meet the mechanical design requirements of this case because there is no intersection between the functional FER and structural FER. Whereas, the intersection of functional FER and structural FER of aluminum indicates that it can fulfill the requirements of both functionality and structure simultaneously. Therefore, we selected aluminum for the construction of this case's mechanism. According to Figure 4b, the selected aluminum rod has a cross-sectional moment of inertia of 19.042 mm^4, resulting in

a circular diameter of 4.4 mm. The aluminum rod with a cross-sectional diameter of 4.4 mm should be selected as the manufacturing material for the mechanism in this case. Taking the electromagnetic-assisted unmanned aerial vehicle (UAV) as an example, the motion trajectory curve of the UAV is obtained through mathematical calculations and program design (as shown in Figure 4c, d, e and f). Additionally, the result plot using copper material as the selected material is also depicted to validate the correctness of the design process.

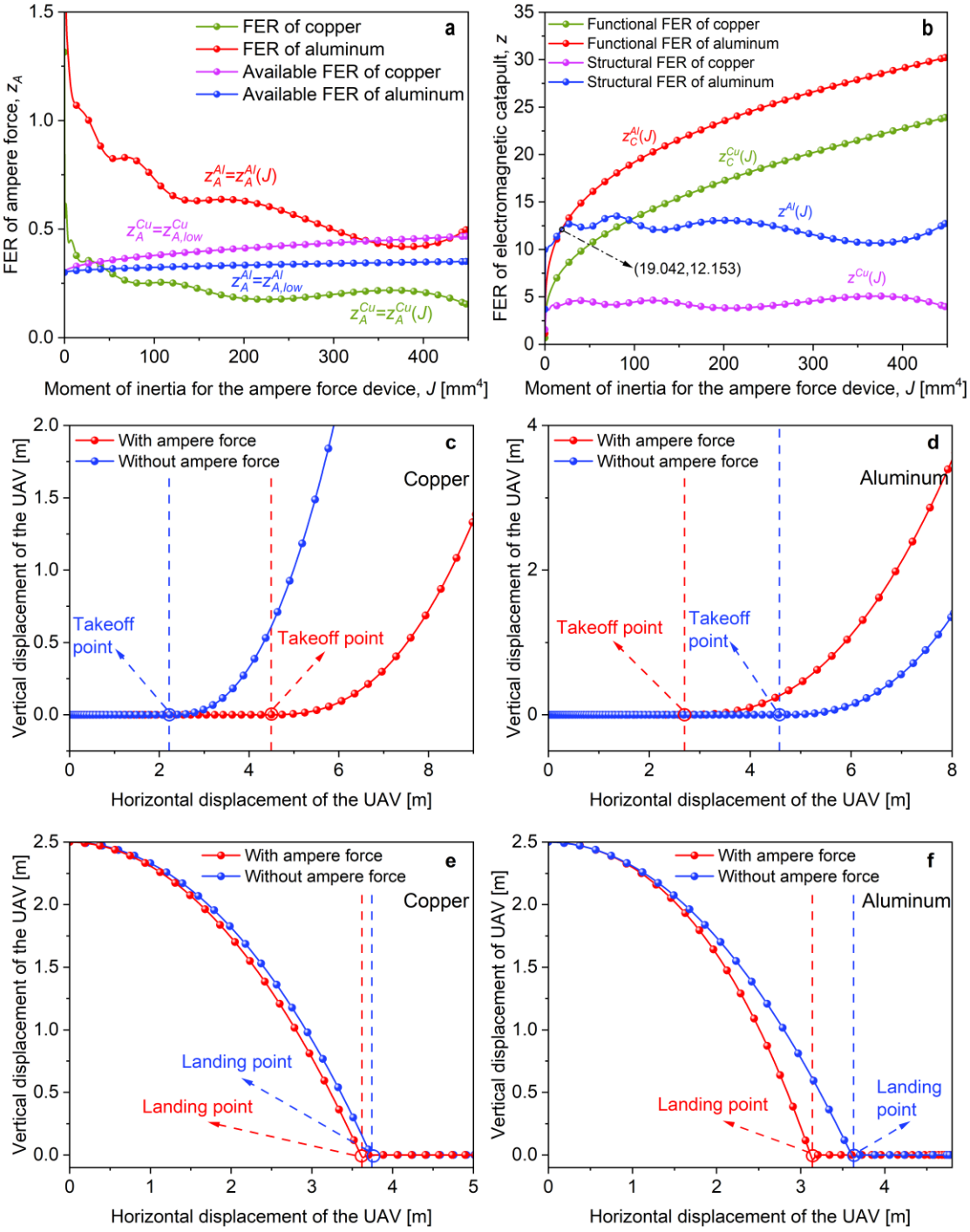

Figure 4. a represents the FER curves of the mechanism; **b** represents the functional and structural FER curves of the mechanism; **c** represents the takeoff trajectory of copper; **d** represents the landing trajectory

of copper; **e** represents the takeoff trajectory of aluminum; **f** represents the landing trajectory of aluminum. It can be seen from the results that during the takeoff phase, the takeoff distance of copper under electromagnetic boost conditions is almost twice that of none, while the takeoff distance of aluminum under electromagnetic boost conditions is half compared with that of none. And in the landing phase, both copper and aluminum can shorten the landing distance of UAVs, but the effect of aluminum is better than that of copper.

The analysis of Figure 4c indicates that when copper is employed in this case's design, the UAV exhibits superior acceleration performance without the assistance of ampere forces compared to the ampere force-assisted UAV. Without the assistance of ampere forces, the takeoff distance is approximately 2.22 meters. However, with the aid of ampere forces, the takeoff distance increases to around 4.38 meters, nearly twice the former value. In other words, even though Figure 4e indicates a reduction in the landing distance of the UAV, copper is still not a suitable multi-field coupling material for this case. This demonstrates the validity of the previous analysis utilizing FER conservation in this work. Additionally, according to Figure 4d, in the case of aluminum used in this design, the takeoff distance is approximately 4.58 meters without the assistance of ampere forces. However, with the aid of ampere forces, the takeoff distance is reduced to around 2.7 meters, resulting in a reduction of approximately 41%. This signifies that aluminum enables the successful implementation of the mechanism in this case. Furthermore, based on Figure 4f, the improvement in the landing distance of the UAV is significantly greater when aluminum is selected compared to copper. This aligns perfectly with the experimental findings, indicating that the proposed FER conservation method in this article is indeed capable of evaluating the performance of integrated application materials under multi-field coupling conditions. Furthermore, the materials selected based on this criterion can ensure the success of the mechanism design.

Conclusion

This study presents a micro-scale mechanism and its corresponding macroscopic conservation description, namely FER conservation, for multi-field coupling. This conservation description encompasses known forms of conservation and encompasses the coupling between all possible forms of physical fields. By utilizing FER conservation, we have not only established a universal mathematical and physical model for the fields of thermoelectric and electromechanical materials, but also applied a new parallel design approach in current engineering hot topics, electromagnetic launching of UAV. The validation of these examples indicates that the FER is widely applicable.. This work encourages a future exploration, to establish a universal mechanism for the cross-scale theory of micro-to-macroscopic FER conservation within the framework of modern physics [20].

References

[1]. Chen B. et al., Texture of Nanocrystalline Nickel: Probing the Lower Size Limit of Dislocation

Activity[J]. ***Science***, 2012, 338: 1448-1451. https://doi.org/10.1126/science.1228211.

[2]. Kürnsteiner, P., Wilms, M. B., Weisheit, A. et al. High-strength Damascus steel by additive manufacturing[J]. ***Nature***, 2020, 582: 515–519. https://doi.org/10.1038/s41586-020-2409-3.

[3]. Hinterleitner B., Knapp I., Poneder M. et al. Thermoelectric performance of a metastable thin-film Heusler alloy[J]. ***Nature*** 576, 85–90 (2019). https://doi.org/10.1038/s41586-019-1751-9.

[4]. Min B. et al. Efficient, stable solar cells by using inherent bandgap of α-phase formamidinium lead iodide[J]. ***Science***, 2019, 366: 749-753. https://doi.org/10.1126/science.aay7044.

[5]. Huilong Hou et al. Fatigue-resistant high-performance elastocaloric materials made by additive manufacturing[J]. ***Science***, 2019, 366: 1116-1121. https://doi.org/10.1126/science.aax7616.

[6]. Yang Y., Chen T., Tan L. et al. Bifunctional nanoprecipitates strengthen and ductilize a medium-entropy alloy[J]. ***Nature***, 2021, 595: 245–249. https://doi.org/10.1038/s41586-021-03607-y.

[7] Jiang J., Zhang L., Ming C. et al. Giant pyroelectricity in nanomembranes[J]. ***Nature*****,** 2022, 607: 480–485. https://doi.org/10.1038/s41586-022-04850-7.

[8] Lheritier P., Torelló A., Usui T. et al. Large harvested energy with non-linear pyroelectric modules[J]. ***Nature*****,** 2022, 609: 718–721. https://doi.org/10.1038/s41586-022-05069-2.

[9] Yue P., Xiao J., Xu K. et al. Mathematical model and analysis method for flowfield separation and transition[J]. ***Physics of Fluids***, 2021, 33:044116. https://doi.org/10.1063/5.0047401.

[10]. Li Z., Wang Y., Ma M. et al. Ultrastrong conductive in situ composite composed of nanodiamond incoherently embedded in disordered multilayer graphene[J]. ***Nat. Mater.***, 2023, 22: 42–49. https://doi.org/10.1038/s41563-022-01425-9.

[11] Zhang H., Pryds N., Park D. et al. Atomically engineered interfaces yield extraordinary electrostriction[J]. ***Nature***, 2022, 609: 695–700. https://doi.org/10.1038/s41586-022-05073-6.

[12]. Jin H., Weissmüller J. A material with electrically tunable strength and flow stress[J]. ***Science***, 2011, 332: 1179-1182. https://dOI:10.1126/science.1202190.

[13] Boukai A., Bunimovich Y., Tahir-Kheli J. et al. Silicon nanowires as efficient thermoelectric materials[J]. ***Nature***, 2008, 451, 168–171. https://doi.org/10.1038/nature06458.

[14] Mao J., Chen G. & Ren Z. Thermoelectric cooling materials[J]. ***Nat. Mater***, 2021, 20: 454-461. https://doi.org/10.1038/s41563-020-00852-w.

[15]. Hochbaum A., Chen R., Delgado R. et al. Enhanced thermoelectric performance of rough silicon nanowires[J]. ***Nature***, 2008, 451: 163–167. https://doi.org/10.1038/nature06381.

[16] Biswas K., He J., Blum I. et al. High-performance bulk thermoelectrics with all-scale hierarchical architectures[J]. ***Nature***, 2012, 489: 414–418. https://doi.org/10.1038/nature11439.

[17] Zhao L., Lo S., Zhang Y. et al. Ultralow thermal conductivity and high thermoelectric figure of merit in SnSe crystals[J]. ***Nature*****,** 2014, 508: 373–377. https://doi.org/10.1038/nature13184.

[18] Hinterleitner B., Knapp I., Poneder M. et al. Thermoelectric performance of a metastable thin-film Heusler alloy[J]. ***Nature***, 2019, 576: 85–90. https://doi.org/10.1038/s41586-019-1751-9.

[19] Masato H., Emi M., Motoaki H., Shuichi M. Phonon angular momentum induced by the temperature gradient[J]. ***Phys. Rev. Lett.***, 2018, 121: 175301. https://doi.org/10.1103/PhysRevLett.121.175301.

[20] Francisco J., Cristiano C., Thomas W. Manipulating matter by strong coupling to vacuum fields[J]. ***Science***, 2021, 373(6551). https://doi.org/10.1126/science.abd0336.